Exposing biomolecular properties one molecule at a time

Elmalk, A.

Citation

Elmalk, A. (2012, December 13). *Exposing biomolecular properties one molecule at a time. Casimir PhD Series*. Retrieved from https://hdl.handle.net/1887/20273

Cover Page

Universiteit Leiden

The handle http://hdl.handle.net/1887/20273 holds various files of this Leiden University dissertation.

Author: Elmalk, Abdalmohsen
Title: Exposing biomolecular properties one molecule at a time
Date: 2012-12-13

Chapter 3

Probing redox proteins on a gold surface by single molecule fluorescence spectroscopy[†]

Summary. *The interaction between the fluorescently labeled redox protein, azurin, and a thin gold film is characterized using single-molecule fluorescence intensity and lifetime measurements. Fluorescence quenching starts at distances below 2.5 nm from the gold surface. At shorter distances the quenching may increase up to 80% for direct attachment of the protein to bare gold. Outside of the quenching range, a four-fold enhancement of the fluorescence is observed with increasing roughness of the gold layer. Fluorescence-detected redox activity of individual azurin molecules, with a lifetime switching ratio of 0.4, is demonstrated for the first time close to a gold surface.*

3.1. Introduction

Redox reactions drive a plethora of biological and chemical processes ranging from photosynthesis and respiration to industrial catalysis and the operation of fuel cells [1, 2]. Recently, due to their unique properties redox proteins have gained strong interest because of possible applications in biomolecular electronics and biosensing. However, to manipulate single redox proteins and attach them to an electrode surface without affecting their biochemical activity is a challenge. Gold has been used extensively for this purpose as it has a higher surface stability than other metals or non-metallic electrodes, while the surface chemistry of gold is well understood [3-5].

To monitor the activity of redox proteins under single-molecule conditions, it is necessary to maximize sensitivity and specificity. Our recent research efforts have targeted the implementation of a novel fluorescence method allowing single-molecule observation of redox events with enhanced sensitivity [6-9]. Optical tracking of electrochemical events made it possible to determine the electrochemical parameters and redox activity of ensembles of as few as 100 protein molecules [10-12]

For the combination of fluorescent redox state detection and electronic control the protein together with its fluorescent label needs to be placed close to an electrode, usually a metal surface. This raises questions about the fluorophore-metal interaction. The subject has raised considerable interest in recent years because of fundamental and application-oriented reasons [13]. The effect of a metal surface on a nearby fluorophore can lead to both enhancement and quenching of the fluorescence [14-24].

A striking aspect of the fluorophore-metal interaction is its strong and complicated distance dependence. At values of d (where d is the distance between the fluorophore or dye and the metal surface) that are comparable to the wavelength of the exciting light ($d > 500$ nm), interference occurs (both positive and negative) between light emitted in a direction away from the metal surface and light emitted towards the metal surface and reflected off it [24-26].

At intermediate ranges (10 nm < d < 500 nm), the interaction of the molecular transition dipole with the nearby metal surface plasmons can lead to quenching of the emission as well as to enhanced excitation rates [18, 20, 26]. At very close ranges (d < 10 nm), a surface energy transfer model (SET) has been proposed as a quenching mechanism. SET denotes the energy transfer from an oscillating dipole to the free conduction electrons of the metal [27, 28]. It has been found that the quenching efficiency is proportional to $1/d^{-3}$ [18, 24, 26, 29]. Even at these very small distances enhancement of the excitation rate can occur, especially for rough metal surfaces. This is the regime that we focus on.

We studied the fluorescence of labeled redox proteins immobilized on coated glass or on gold films (bare or coated with a self-assembling monolayer (SAM)) as a function of the thickness of the gold film and the thickness of the SAM. Intensity and lifetime measurements allowed for the separation of enhancement and quenching effects on the fluorescence. In addition, the effect of the redox state on the fluorescence of the labeled protein was investigated. While this effect has been successfully studied for the enzyme nitrite reductase (NiR) at the single molecule level [7], the influence of a nearby Au layer has not been reported so far.

The results of the present study are of relevance for the implementation of redox proteins in bio-optoelectronic (nano)devices. To the best of our knowledge, this study is the first successful attempt to examine the single molecule fluorescence lifetimes of labeled redox proteins immobilized on a metal surface.

3.2 Experimental Methods

Protein labeling. Azurin from *Pseudomonas aeruginosa* was used as a redox protein model. It is a small (M_r=14.6 kDa) blue copper protein that functions as an electron carrier possibly in the oxidative stress response of the organism[30]. The intense 600 nm absorption band of this protein in the oxidized state is absent in the reduced state, which makes it suitable for redox state detection by fluorescent labeling. A covalently attached fluorescent label and the redox cofactor (the Cu center) form a FRET pair by which a change in redox state is reflected by a change in fluorescence intensity and fluorescence lifetime [7, 8, 31, 32].

Preparation and purification of the K27C azurin variant was done as previously described [32]. The protein was labeled by incubation of a solution of 0.5 mM protein in 20 mM Hepes, pH 8.3, with a 5 times molar excess of Atto-655 succinimidyl ester (ATTO-TEC GmbH, Germany) for 1 h at room temperature for N-terminal labeling. The unbound dye was removed using centrispin-10 columns (Princeton Separations; Adelphia, NJ,

USA). Labeled protein was diluted with 20 mM Hepes buffer, pH 7.0, to the desired final concentrations as determined by UV-vis spectroscopy.

Preparation of surfaces. All glass slides (Menzel, Germany) used to prepare gold films and silanized glass were sonicated in spectrometer grade acetone (30 min), washed several times with water (Millipore water), dipped in 10% $NaOH/H_2O$ (30 min), washed again several times with water and stored in methanol. Before use the cover slips were dried and ozone-cleaned (UVP PR-100 UV-ozone photoreactor) for 1 h immediately before silanization or sputtering.

For the preparation of gold films, first, a 1 nm thick adhesion layer of molybdenum-germanium (MoGe) films was prepared by depositing MoGe onto freshly cleaned glass slides by magnetron sputtering using an ATC 1800-F system (AJA corporation). The MoGe films were sputtered with a deposition rate of 1.32 nm/min (10 mTorr Argon environment). Second, gold films of specified thickness were prepared by sputtering at a deposition rate of 9.06 nm/min (10 mTorr environment composed of a mixture of argon with 1% oxygen) on top of the MoGe film. The Au films were used immediately after preparation. Their thickness was varied between 10 and 100 nm.

Atomic force microscopy. Atomic force microscopy (AFM) imaging of the samples was performed with a commercial AFM microscope (Nanoscope IIIa, Veeco, USA). Tapping mode images in air were acquired with an E-scanner (14 μm range), using Si probes with a resonance frequency of 75 kHz and a nominal spring constant of 2.8 N m^{-1}.

Protein immobilization. In one type of experiment the labeled protein was immobilized on a glass slide or a sputtered bare gold surface for optical measurements. Immobilization in the former case was achieved by depositing a layer of a 100:1 mixture of triethoxysilane (TES) and mercaptopropyl trimethoxysilane (MPTS) on a cleaned glass slide (chemicals from Fluka, used as received). The K27C azurin was bound to the silanized glass through a 1–11-bismaleimidotetraethyleneglycol linker (BM(PEO)₃, Pierce) as described by Kuznetsova et al. [7]. Immobilization on bare gold was realized by incubating the Au film with a solution of the K27C azurin overnight at room temperature and rinsing the surface afterwards by flushing with buffer. This gave reproducible results of specifically immobilized K27C azurin without protein aggregation at the surface.

In a second type of experiment mixed SAMs of 1,n-alkanedithiol $HS(CH_2)_nSH$ ($n= 4, 6, 8$ and 10) and OH-terminated alkanethiol $HS(CH_2)_mOH$ ($m = n\text{-}2$, except for $n=4$ in which case we chose $m=3$), denoted by Cnd ('d' denoting di-thiol), were prepared by immersing slides with freshly sputtered Au films into a 2-propanol solution containing a mixture of $HS(CH_2)_mOH$ (10 mM) and $HS(CH_2)_nSH$ (1 mM) overnight at room temperature [33] (all

chemicals purchased from Aldrich Chemicals, dissolved in 2-propanol). The choice for n>m, *i.e.*, for an alkanedithiol that is longer than the OH-terminated alkanethiol, was made to expose the reactive thiol of the linker. It provides the reaction site for immobilization of the K27C azurin, while the OH-terminated alkanethiol serves as the diluant to control the density of immobilized protein, as it prevents non-specific binding of K27C azurin (Fig. 1). Au slides were removed from solution, rinsed extensively with 2-propanol, and dried in a pure N_2 flow. A 200 pM solution of the labeled azurin (Az) in 20 mM Hepes buffer, pH 7, was deposited onto the SAM-covered Au slide and left to incubate overnight at 4°C. The slide was then rinsed with 20 mM Hepes buffer (pH 7) to remove free azurin. Measurements were performed in the same 20 mM Hepes buffer (pH 7) as used for immobilization.

In all experiments reduction was performed with sodium ascorbate, oxidation was performed by adding potassium ferricyanide. Reducing and oxidizing agents were added from freshly prepared stock solutions to final concentrations of 10mM sodium ascorbate or 1 mM potassium ferricyanide. The thickness of the sputtered Au films was varied between 10 and 100 nm.

The success of the immobilization procedure was verified using tapping mode AFM (Figures S1 and S2 in the supplementary material of reference 34)[34]. For the mixed alkanedithiol/OH-alkanethiol SAMs, distinct features with a height of 4.0±0.2 nm were observed. This value corresponds with the size of azurin (3.5 x 3.5 x 4.4 nm^3) as determined by X-ray crystallography [35]. As a control for the specificity of the attachment
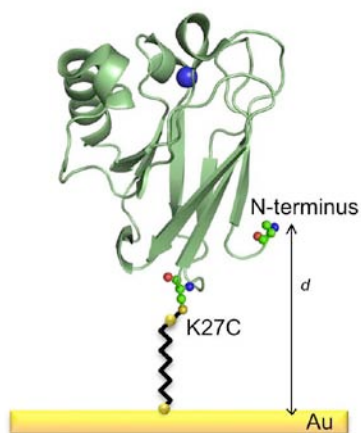

Figure 1. Representation of the azurin (K27C) structure and schematic view of the covalent coupling of azurin to a SAM-modified Au surface. The distance *d* between the dye label at the N-terminus and the Au surface is indicated.

on the SAM, azurin was incubated on a SAM of 8-mercapto-1-octanol only, applied on a 20 nm Au film. No protein was found on this surface after rinsing with pure buffer solution. The immobilization strategy described above, thus, establishes an effective and specific coupling between the protein and the gold surface [3, 36-38].

Table 1. Root-mean square (rms) values of height variations for various Au films, as determined by AFM.

Au thickness (nm)	rms (nm)
10	0.2
20	0.3
50	1.4
100	1.7

The change of surface morphology of the gold film with increasing thickness was also characterized by AFM. Calculated roughness values are given in Table 1. Thin sputtered gold films (10 nm) have root-mean square (rms) height variations of about 0.2 nm. With increasing thickness of the Au film, the roughness goes up, reaching 1.7 nm rms value at 100 nm thickness. The thin Au films exhibit an exceptionally smooth and homogenous surface due to the presence of the MoGe wetting layer. At thicknesses above 20 nm the effect of the wetting layer diminishes and the surface roughness of thick Au films has a value more typical of a sputtered metal surface.

Confocal microscopy. The fluorescence measurements were conducted on a home-built sample scanning confocal microscope. For fluorescence excitation a pulsed picosecond diode laser (PDL 800-B, PicoQuant GmbH) with an output wavelength of 639 nm was sent through a narrow-band clean-up filter (LD01-640/8-25, Semrock, USA), coupled into a single-mode fiber and reflected by a dichroic mirror (Z 532/633 M, Chroma technology, USA) to a high numerical aperture oil objective (100× oil, NA 1.4, Zeiss, Germany) and focused to a diffraction-limited spot (~300 nm) on the sample surface. The power density at the sample was 0.5–1 kW/cm^2. Epi-fluorescence from the labeled azurin was filtered with a band filter (D 675/50 M, Chroma technology, USA) and focused with a +45 mm focal length achromatic lens on to the active area of a single photon avalanche photodiode (Perkin-Elmer SPCM-AQR-14). The microscope was equipped with Time-Correlated Single-Photon Counting (TCSPC) capabilities. The data acquisition was done by the TimeHarp 200 TCSPC PC-board operating in the special Time-Tagged Time-Resolved (T3R) mode, which stores the arrival time of each individual photon event [39]. Samples were
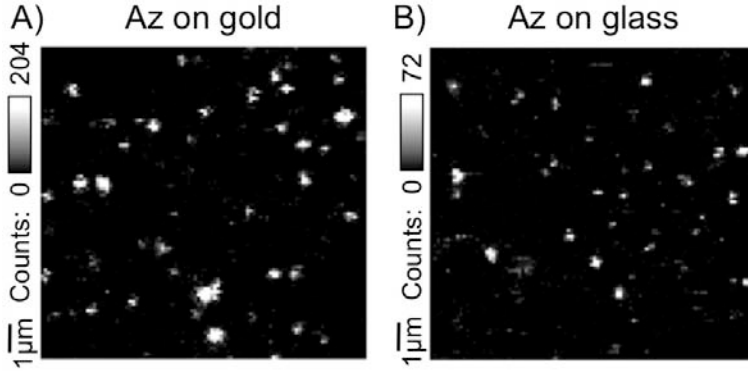
Figure 2. 10x10 µm^2 fluorescence images of immobilized K27C azurin (20 mM Hepes buffer, pH 7). A) on a 100nm Au film coated with C10d SAM. B) on glass. The scale bars show the intensity counts in 1.8 msec bin time. The fluorescence intensities of individual spots on the 100 nm coated Au film are brighter than on glass (notice different scale bars).

mounted onto a Physik Instrumente P-517 nanopositioner. Scanning, accurate positioning, data collection and analysis were performed by the Picoquant SymPho-Time software (PicoQuant GmbH).

The excitation beam was focused through (transmissive mode) or impinged on (direct mode) the gold films in order to excite the molecules on the surface. The direct mode was used for the Au films with a thickness of 20 nm and higher, because they are not transparent. For thicknesses of 10 and 15 nm the transmissive mode of detection was compared to the direct mode, using the same sample in both geometries. Identical results were obtained in both cases.

Life time analysis. The fluorescence intensity decays were analyzed as the sum of mono-exponential decays [40]:

$$I(t) = \sum_{i=1}^{n} \alpha_i \exp(-t / \tau_i) , \qquad [1]$$

where τ_i are the decay times and α_i are the amplitudes. The contribution of each component to the average intensity is given by

$$f_i = \frac{\alpha_i \tau_i}{\sum_j \alpha_j \tau_j} . \qquad [2]$$

49

The average lifetime of the multi- exponential decay is defined by

$$\overline{\tau} = \sum_i f_i \tau_i \; .$$ [3]

The values of α_i and τ_i were determined using the PicoQuant SymPho-Time software. The data are fitted with a convolution of the instrument response function (IRF) and a sum of exponential decays according to a least-squares criterion [41].

3.3 Results

3.3.1 Fluorescence intensity vs. film thickness

To investigate the effect of **Au film thickness** on the **fluorescence** of labeled azurin, a single-molecule fluorescence experiment was carried out on labeled K27C Az immobilized on Au films of different thicknesses, coated with a C*10*d mixed SAM (no fluorescence quenching occurs for this SAM; vide infra). A characteristic confocal image (10 by 10 µm) of individual reduced azurin molecules on 100 nm thick Au film coated with C*10*d SAM (in buffer) is shown in Fig. 2A. For comparison, we also recorded a confocal fluorescence image of labeled azurin molecules on a glass surface, see Fig. 2B. As can be seen from the scale bars in Fig. 2, there is a difference in fluorescence intensity of roughly a factor of 3-4.

In order to quantitatively compare the fluorescence properties for different azurin molecules and explore the underlying photophysics, we monitored the fluorescence of individual azurin molecules. A typical fluorescence time trace of a single, labeled azurin
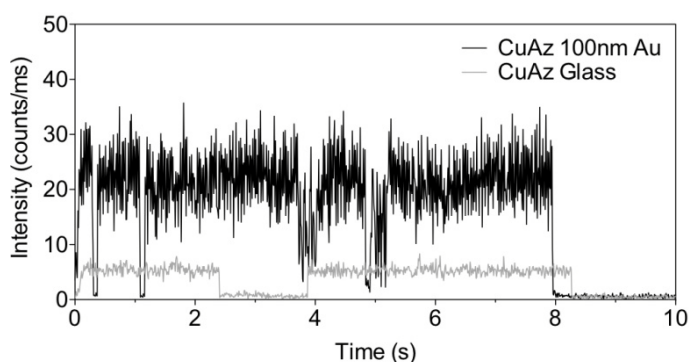
Figure 3. Fluorescence time traces obtained from immobilized reduced Cu-Az (K27C azurin) on 100 nm Au film coated with C*10*d SAM (black) and from reduced Cu-Az on a glass surface (gray).

molecule on a 100 nm Au film coated with a C*10*d mixed SAM is shown in Fig. 3, which corresponds to a four-fold higher fluorescence emission rate than that of azurin on glass (Fig. 3).

In Fig. 4, count rate histograms of collections of individual molecules are shown for azurin on glass and on C*10*d coated Au films, the latter with thicknesses of 20 nm, 50 nm and 100 nm. All measurements were carried out at the same laser intensity of 1 kW/cm^2. The count rate distribution of azurin immobilized on 50 and 100 nm Au films is strongly bimodal,
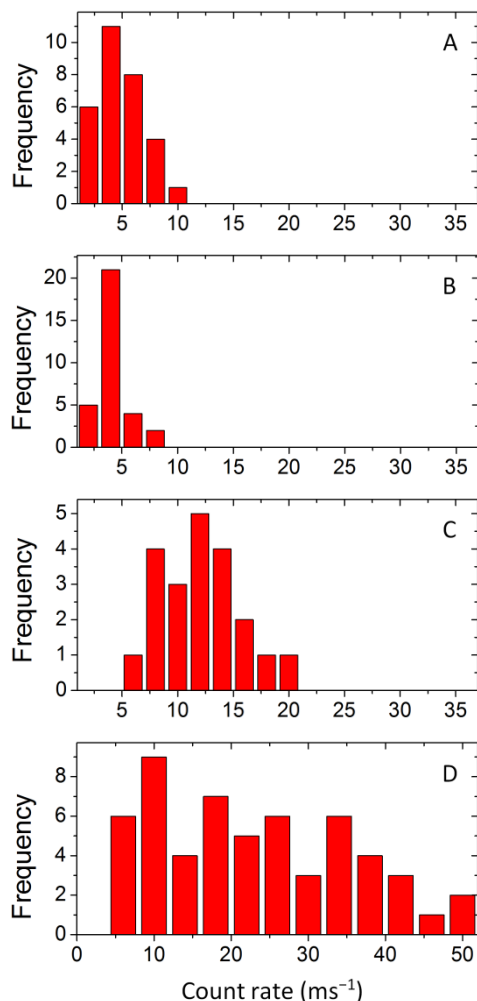

FIG. 4. Intensity count rate histograms for reduced K27C azurin molecules immobilized on silanized glass (A) and on Au films (B: 20 nm, C: 50 nm and D: 100 nm thickness) coated with a C*10*d SAM.

with maxima at 6 and 25 counts/ms. The former count rate is similar to the fluorescence count rate of labeled azurin on glass and on gold films with a thickness of 10 and 20 nm. The high count rate of what is by far the largest fraction (80%) of azurin molecules on 50 and 100 nm Au films suggests a strong fluorescence enhancement as compared to azurin molecules immobilized on glass or 10 and 20 nm Au films. The average enhancement for azurin on 50 and 100 nm Au films as estimated from the count rate histograms in Fig. 4 is four-fold.

The main difference between the thick (50 and 100 nm) and the thin (10 and 20 nm) Au films is the surface roughness (see Table 1). Apparently, the fluorescence enhancement strongly depends on this particular property. In general, the fluorescence near metal surfaces is governed by the distance-dependent competition between quenching and (local-field) enhancement [16, 23]. These aspects were examined in more detail by means of lifetime measurements.

3.3.2. Fluorescence life time vs. SAM thickness

When immobilizing proteins on a SAM-coated Au film the SAM layer constitutes a spacer between the bare gold surface and the protein. By using a series of *n*-alkanedithiols with lengths ranging from 4 to 10 carbon atoms the effect of a **SAM thickness** variation of from 5.9 to 12.5 Å [37, 42-44] on the **fluorescence lifetime** could be studied. The results are shown in Fig. 5 for a 50 nm thick Au film. Fluorescence decays were averaged over more than 500
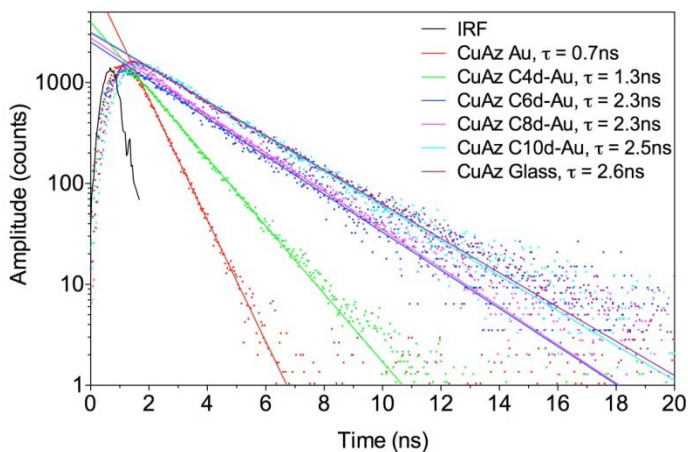

FIG. 5. Fluorescence decay curves of azurin immobilized on glass (purple), immobilized directly on 50 nm Au film (red) and on 50 nm Au films coated with C*4*d (green), C*6*d (blue), C*8*d (magenta) or C*10*d (cyan). IRF (black) is also included. Each decay curve represents an average over more than 500 individual molecules.

single-molecule traces and quantified by fitting to mono-exponential decays convoluted with the instrument response function (IRF). Reduced azurin immobilized on C*10*d, the thickest SAM used, shows approximately the same lifetime as reduced azurin on glass (2.5 resp. 2.6 ns). Significantly reduced lifetimes are observed for the shorter SAMs (C*8*d, C*6*d and C*4*d with lifetimes of 2.3, 2.3 and 1.2 ns respectively), down to 0.7 ns for azurin immobilized directly on Au, see Table 2.

To verify that the observed lifetimes were not affected by redox effects, the experiments were repeated with Zn azurin, which is redox-inactive. The lifetimes were similar to those observed for Cu-azurin. This confirms that the decrease in lifetime is not due to a redox-state dependent interaction between Cu site and dye label [31]. We suggest that the reduced lifetime at shorter distances reflects the fluorescence quenching by molecule-metal interactions. Notably, labeled azurin molecules bound to C*10*d SAM seem to be at a distance which is sufficiently large to prevent fluorescence quenching. Nevertheless, the thickness of this SAM is only 1.3 nm [42]. Apparently, the probed interaction is very short-ranged.

3.3.3 Fluorescence life time vs. Au film thickness

In order to examine the effect of the Au film **thickness** on the **fluorescence lifetime**, the measurement series described above was repeated for Au films with thicknesses of 10, 20, 50 and 100 nm. The fluorescence data were all collected under the same excitation and detection conditions, allowing a direct comparison between the different measurements (Fig. 6). The fluorescence lifetime is found to be completely independent of the Au film thickness, from which it is concluded that the morphology of the Au surface does not affect the degree of fluorescence quenching.

TABLE II. Fluorescence lifetimes of azurin immobilized on glass and on 50 nm Au films coated with SAMs of varying thicknesses.

SAM	τ (ns) [b]
___ [a]	0.7±0.1
C4d	1.3±0.1
C6d	2.3±0.1
C8d	2.3±0.1
C10d	2.5±0.1
Glass	2.6±0.1

a) azurin immobilized directly on bare Au; no SAM;.
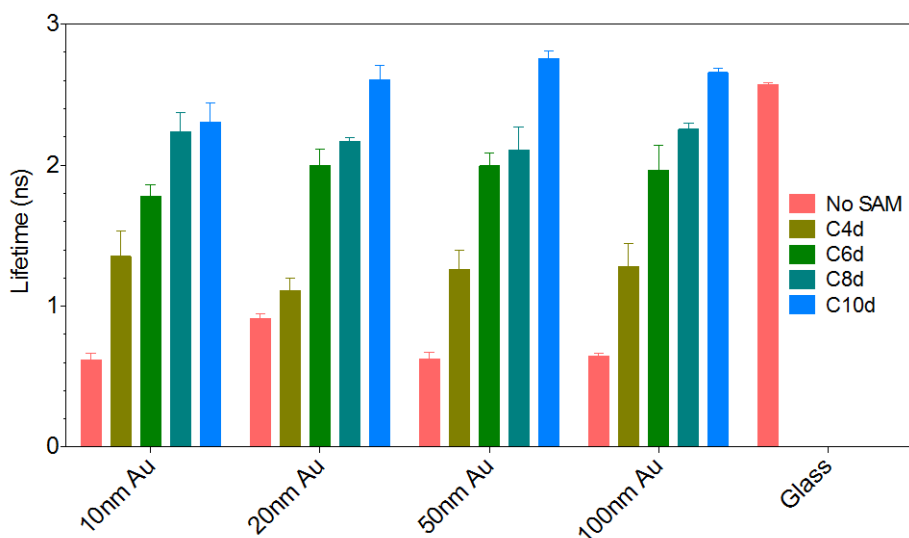b) fluorescence lifetime.

FIG. 6. Fluorescence lifetimes of reduced Cu-Az immobilized on Au films of different film thicknesses (from 10 to 100 nm) that are coated with C*4*d (olive), C*6*d (green), C*8*d (blue-green) and C*10*d (bright blue) SAMs and of reduced Cu-Az adsorbed directly on 50 nm Au (red). Also presented is the lifetime of reduced Cu-Az immobilized on silanized glass (red). The lifetimes were obtained by monitoring the total emission of a 10x10µm^2 surface area. For each bar the lifetimes measured for a number of pictures (varying from 2 to 16) were averaged. The error bars correspond to standard deviations.

Thus, the fluorescence lifetime only depends on the distance between fluorophore and Au surface, independent of film thickness. The shortest fluorescence lifetimes were observed when azurin was adsorbed directly on the Au films, which is to be expected as quenching is known to be stronger at shorter distance. The lifetime of azurin bound to C*10*d is the longest and similar to the lifetime of azurin on glass. Interestingly, azurin bound to C*6*d and C*8*d shows similar lifetimes, suggesting that different SAM chain lengths do not always lead to different SAM thicknesses.

In conclusion it can be stated that, whereas the fluorescence *lifetime* is independent of Au film thickness, the fluorescence *intensity* does depend on it (see Fig. 4). Clearly, two different mechanisms play a role.

3.3.4 Effect of redox state

The experiments reported so far relate to azurin in the reduced state. To check how the redox state of the protein might affect the fluorescence behavior, we also measured the fluorescence intensity and lifetime for azurin in the oxidized state. The redox state could be
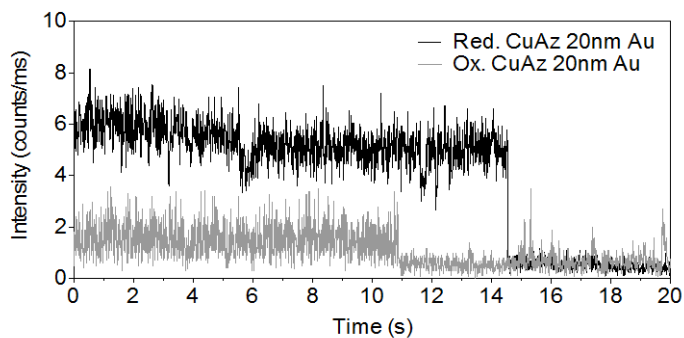
Fiure 7. Time traces for two individual labeled K27C azurin molecules immobilized on a 20 nm Au film coated with C*10*d SAM, one trace for azurin in the reduced state (black, $\tau_{red} = 2.6$ nsec), and one for azurin in oxidized form (gray, $\tau_{oxid} = 1.6$ nsec).

easily controlled by the addition of reducing or oxidizing agents (see above). Figure 7 shows time traces for two individual azurin molecules immobilized on a 20 nm Au film coated with C*10*d SAM, one in the reduced state (black), and one in oxidized form (gray). The intensity ratio between the two states is about a factor of 3 in this instance.

Lifetime histograms are shown in Fig. 8 for oxidized (bottom, left) and reduced (bottom, right) single azurin molecules bound to C*10*d SAM on 20 nm Au films, which appear
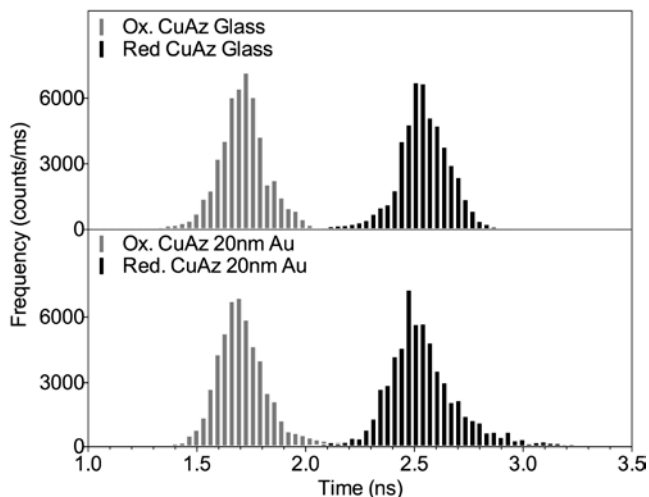
FIG. 8. Fluorescence lifetime histograms of labeled K27C azurin in the oxidized (histograms at the left) and the reduced state (histograms at the right) immobilized on 20 nm Au coated with a C*10*d SAM (bottom) and immobilized on glass (top).

similar to azurin on glass surfaces (top). Reduced and oxidized molecules exhibit a long (2.6±0.2 ns, black bars) and a short lifetime (1.6±0.2 ns, gray bars), respectively. The oxidized azurin lifetimes were found to be independent of the Au film thickness, just as for reduced azurin. For azurin immobilized on a C8d SAM on Au films of varying thicknesses the reduced and oxidized forms exhibited lifetimes of 2.3±0.2 ns and 1.1±0.2 ns, respectively. Thus, it is still possible to discern the two redox states in the presence of fluorescence quenching by a metal surface. Lifetimes were also measured for oxidized azurin immobilized on C6d and C4d SAMs and on bare Au. The results exhibit the same trend as the distance dependent fluorescence quenching data observed for reduced azurin.

3.4 Discussion

In the following we discuss the distance dependence of the fluorescence quenching, the relation between fluorescence enhancement and surface roughness, and the redox switching behavior.

Both quenching and enhancing interactions between fluorophores and metal surfaces have an effect on the fluorescence intensity and lifetime. The fluorescence intensity (below saturation) is proportional to the fluorescence emission rate γ_{em}, which is the product of the excitation rate γ_{exc} and quantum yield q [15] :

$$\gamma_{em} = \gamma_{exc} q \,. \tag{4}$$

In the absence of a metal surface, the free-space quantum yield q_0 is given by:

$$q_0 = \left(\gamma_r \Big/ \gamma_r + \gamma_{nr} \right), \tag{5}$$

where γ_r is the radiative rate and γ_{nr} the (intrinsic) nonradiative decay rate of the molecule. When the fluorophore is placed near the metal surface, both the excitation rate γ_{exc} and the quantum yield q are modified by the fluorophore-metal interaction [15, 16, 45]. Especially on rough surfaces, γ_{exc} may be increased due to the enhanced local electric field near the metal surface. Interaction of the molecular transition dipole moment with such an enhanced local field may also lead to an increase in the radiative decay rate. An increase in γ_{exc} and/or γ_r will result in an increased emission rate and hence an enhanced fluorescence intensity, but only a change in γ_r will affect the excited state lifetime.

At the very close ranges probed here (fluorophore-metal distance $d < 10$ nm), so-called surface energy transfer (SET) takes place from the excited molecule to the free conduction electrons of the metal. This introduces an additional non-radiative channel (which partly

quenches the fluorescence) with rate γ_{set} [16]. As a consequence, the modified quantum yield can be written as

$$q = \gamma_r \Big/ \gamma_r + \gamma_{nr} + \gamma_{set} \, .$$ [6]

For transfer to a metal occupying the half-space below the dipole, γ_{set} is proportional to $1/d^3$ [18, 24]. This also applies to thin films as long as they are much thicker than d, which is the case here.

The competition between the increase of the excitation rate γ_{exc}, the increase of the radiative rate γ_r, and the increase of γ_{set}, which enhances fluorescence quenching, becomes highly significant in the sub-5 nm distance range studied here. We believe that γ_r is not affected in our measurements. This can be concluded from the complete decoupling in our data between the lifetime changes (which only occur for a change in SAM thickness) and the intensity enhancement (which only occurs with a change in Au film thickness). The lifetime is given by

$$\tau = 1 \Big/ \gamma_r + \gamma_{nr} + \gamma_{set}$$ [7]

while the intensity is proportional to

$$I \approx \gamma_{exc}\gamma_r \Big/ \gamma_r + \gamma_{nr} + \gamma_{set}$$ [8]

Thus, an increase in γ_r would affect both lifetime and fluorescence enhancement at the same time. Since this is not what is observed, only γ_{set} and γ_{exc} change. To monitor changes in γ_{set}, we look at the thinner gold films, for which there is no enhanced excitation, i.e. γ_{exc} is not affected. For the change in γ_{exc} we look at the data for the thickest SAM (C*10*d), for which the lifetime is unchanged compared to Az on glass, and thus γ_{set} must be zero.

The SAM thickness dependence investigation we have carried out showed that fluorescence emission of labeled azurin is quenched significantly at close distances to the gold surface (Figures 5 and 6). This was observed as a fluorescent lifetime reduction when the alkanethiol spacer length was decreased. We suggest that the fluorescence from labeled azurin immobilized on C8d, C6d, C*4*d and labeled azurin directly adsorbed on the Au surface is quenched due to the surface energy transfer process. For this we calculate γ_{set} in terms of the unquenched value (found for the C*10*d SAM) $\gamma_0 = \gamma_r + \gamma_{nr}$, using $\tau_0 = 1/\gamma_0$ and

$$\tau = \frac{1}{\gamma_r + \gamma_{nr} + \gamma_{set}} = \frac{1}{\gamma_0 + \gamma_{set}} \qquad [9]$$

which gives

$$\frac{\gamma_{set}}{\gamma_0} = \frac{\tau_0}{\tau} - 1 \qquad [10]$$

(see Table 3). The relation of γ_{set} to the distance is found to be in agreement with the expected $1/d^3$ dependence (Fig. 9), with d as indicated in Fig. 1.

By varying the Au film thickness the dependence of the fluorescence enhancement on the surface roughness was investigated. The enhancement observed for the 50 and 100 nm gold films is attributed to the change in excitation rate caused by local enhancement of the electromagnetic field of the incident light as it interacts with the rough metal surface [40, 46-50]. Fluorescence enhancement for dye molecules directly deposited on rough metallic surfaces has been reported before, also in the sub-5 nm regime [40, 46, 47, 51]. Our data show that this local field enhancement can lead to an increase in the emission rate γ_{em}, and, thereby, in the emission intensity, without altering the radiative decay rate γ_r or introducing any quenching effects. Such a change in intensity without a change in lifetime has been observed previously for a similar dye-metal system [52]. The presence of two populations
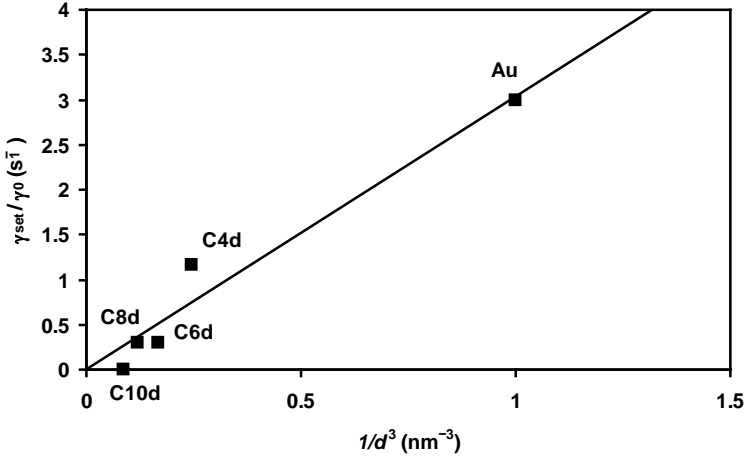

FIG. 9. Dependence of the surface energy transfer rate γ_{set} on the inverse cubic distance, $1/d^3$. The straight line is a linear fit to the data points. Data taken from Table III.

(enhanced and unenhanced emitters, both with the same lifetime, see Fig. 4) is ascribed to the microscopic features of the metal surface. It is well known that the electromagnetic field enhancement depends upon the local surface roughness and the surface morphology [49]. Therefore, local variation in the surface morphology may lead to a variation in the enhancement.

The results on chemical oxidation and reduction of azurin show that the proteins remain redox active on the gold surfaces with the used immobilization strategy. To compare the redox switching as inferred from the intensity time traces and from the fluorescence lifetimes the amount of switching for both types of measurement was calculated. We find the intensity-based switching ratio, Q_I, to be 0.7 with

$$Q_I = 1 - (F_{oxid} / F_{red}) \qquad [11]$$

in which F_{oxid} and F_{red} denote the fluorescence intensity of the Az in the reduced and oxidized form, respectively [31], while the lifetime-based switching ratio [53], Q_L,

$$Q_L = 1 - (\tau_{oxid} / \tau_{red}) \qquad [12]$$

appears to be 0.4. Here, τ_{oxid} and τ_{red} denote the fluorescence lifetime of the Az in the reduced and oxidized form, respectively. The discrepancy between these two values is currently the subject of further investigation.

SAM	d/ nm [a]	q/q$_0$ [b]	γ_{set}/γ_0 [c]
none	1	0.25	3
C4d	1.6	0.46	1.2
C6d	1.8	0.77	0.3
C8d	2.0	0.77	0.3
C10d	2.3	1	0

Table 3. Distance dependence of the fluorescence quantum yield q and the surface energy transfer rate γset.

a) Distance from dye label to gold surface, calculated by increasing the SAM thickness by 1 nm to account for the distance between the label and the SAM layer (see Figure 1). SAM thickness was calculated according to Heering and Canters 39 and Love et al. 37, using a C-C bond length of 1.27 Å, a CS endgroup size of 1.79 Å and a SAM/Au angle of 30°.
b) $q/q_0 = \tau/\tau_0$. Lifetime values taken from Table II; τ0 values refer to C10d data.
c) Calculated from Equation [10].

3.5. Conclusion

In summary, the combination of labeled azurin immobilized on Au with a mixed SAM has enabled us to characterize the label-metal interaction in detail. Fluorescence quenching is shown to be a short range effect, reflecting energy transfer between the fluorophore and conduction electrons of the metal. Significant fluorescence enhancement is observed with increasing roughness of the gold layer. These results are in good agreement with theoretical predictions based on earlier, non-single molecule, experiments with fluorophores on metal films.

The results also illustrate how the redox states of a single protein molecule can be investigated by fluorescence lifetime analysis both for Az on gold and for Az on glass. Thus, the combination of FLIM (fluorescence lifetime imaging) with our FRET-based redox detection method provides a new approach for studying the kinetics of biological electron transfer at the single molecule level. Furthermore, the ability to tune the emission properties of labeled redox proteins immobilized on metal surfaces opens a way to design improved biosensing devices.

Reference List

1. Willner I. Biomaterials for sensors, fuel cells, and circuitry. Science 2002; 298(5602):2407-2408.

2. Gilardi G, Fantuzzi A. Manipulating redox systems: application to nanotechnology. Trends in Biotechnology 2001; 19(11):468-476.

3. Chi QJ, Farver O, Ulstrup J. Long-range protein electron transfer observed at the single-molecule level: In situ mapping of redox-gated tunneling resonance. Proceedings of the National Academy of Sciences of the United States of America 2005; 102(45):16203-16208.

4. Astier Y, Canters GW, Davis JJ, Hill HAO, Verbeet MP, Wijma HJ. Sensing nitrite through a pseudoazurin-nitrite reductase electron transfer relay. Chemphyschem 2005; 6(6):1114-1120.

5. Tepper AWJW. Electrical Contacting of an Assembly of Pseudoazurin and Nitrite Reductase Using DNA-Directed Immobilization. Journal of the American Chemical Society 2010; 132(18):6550-6557.

6. Goldsmith RH, Tabares LC, Kostrz D, Dennison C, Aartsma TJ, Canters GW, Moerner WE. Redox cycling and kinetic analysis of single molecules of solution-phase nitrite reductase. Proceedings of the National Academy of Sciences of the United States of America 2011; 108(42):17269-17274.

7. Kuznetsova S, Zauner G, Aartsma TJ, Engelkamp H, Hatzakis N, Rowan AE, Nolte RJM, Christianen PCM, Canters GW. The enzyme mechanism of nitrite reductase studied at single-molecule level. Proceedings of the National Academy of Sciences of the United States of America 2008; 105(9):3250-3255.

8. Schmauder R, Librizzi F, Canters GW, Schmidt T, Aartsma TJ. The oxidation state of a protein observed molecule-by-molecule. Chemphyschem 2005; 6(7):1381-1386.

9. Tabares LC, Kostrz D, Elmalk, Andreoni A, Dennison C, Aartsma TJ, Canters GW. Fluorescence lifetime analysis of nitrite reductase from Alcaligenes xylosoxidans at the single-molecule level reveals the enzyme mechanism. Chemistry a European Journal 2011; 17:12015-12019.

10. Davis JJ, Burgess H, Zauner G, Kuznetsova S, Salverda J, Aartsma T, Canters GW. Monitoring interfacial bioelectrochemistry using a FRET switch. Journal of Physical Chemistry B 2006; 110(41):20649-20654.

11. Salverda JM, Patil AV, Mizzon G, Kuznetsova S, Zauner G, Akkilic N, Canters GW, Davis JJ, Heering HA, Aartsma TJ. Fluorescent Cyclic Voltammetry of Immobilized Azurin: Direct Observation of Thermodynamic and Kinetic Heterogeneity. Angewandte Chemie-International Edition 2010; 49(33):5776-5779.

12. Krzeminski L, Ndamba L, Canters GW, Aartsma TJ, Evans SD, Jeuken LJC. Spectroelectrochemical Investigation of Intramolecular and Interfacial Electron-Transfer Rates Reveals Differences Between Nitrite Reductase at Rest and During Turnover. Journal of the American Chemical Society 2011; 133(38):15085-15093.

13. Rinaldi R, Biasco A, Maruccio G, Arima V, Visconti P, Cingolani R, Facci P, De Rienzo F, Di Felice R, Molinari E, Verbeet MP, Canters GW. Electronic rectification in protein devices. Applied Physics Letters 2003; 82(3):472-474.

14. Andolfi L, Bruce D, Cannistraro S, Canters GW, Davis JJ, Hill HAO, Crozier J, Verbeet MP, Wrathmell CL, Astier Y. The electrochemical characteristics of blue copper protein monolayers on gold. Journal of Electroanalytical Chemistry 2004; 565(1):21-28.

15. Anger P, Bharadwaj P, Novotny L. Enhancement and quenching of single-molecule fluorescence. Physical Review Letters 2006; 96(11).

16. Bharadwaj P, Novotny L. Spectral dependence of single molecule fluorescence enhancement. Optics Express 2007; 15(21):14266-14274.

17. Chance RR, Prock A, Silbey R. Lifetime of An Emitting Molecule Near A Partially Reflecting Surface. Journal of Chemical Physics 1974; 60(7):2744-2748.

18. Chance RR, Prock A, Silbey R. Comments on Classical Theory of Energy-Transfer. Journal of Chemical Physics 1975; 62(6):2245-2253.

19. Chance RR, Prock A, Silbey R. Comments on Classical-Theory of Energy-Transfer .2. Extension to Higher Multipoles and Anisotropic Media. Journal of Chemical Physics 1976; 65(7):2527-2531.

20. Ford GW, Weber WH. Electromagnetic-Interactions of Molecules with Metal-Surfaces. Physics Reports-Review Section of Physics Letters 1984; 113(4):195-287.

21. Fort E, Gresillon S. Surface enhanced fluorescence. Journal of Physics D-Applied Physics 2008; 41(1).

22. Fu Y, Lakowicz JR. Modification of single molecule fluorescence near metallic nanostructures. Laser & Photonics Reviews 2009; 3(1-2):221-232.

23. Lakowicz JR. Radiative decay engineering 5: metal-enhanced fluorescence and plasmon emission. Analytical Biochemistry 2005; 337(2):171-194.

24. Waldeck DH, Alivisatos AP, Harris CB. Nonradiative Damping of Molecular Electronic Excited-States by Metal-Surfaces. Surface Science 1985; 158(1-3):103-125.

25. Drexhage KH. Influence of A Dielectric Interface on Fluorescence Decay Time. Bulletin of the American Physical Society 1969; 14(8):873-&.

26. Hellen EH, Axelrod D. Fluorescence Emission at Dielectric and Metal-Film Interfaces. Journal of the Optical Society of America B-Optical Physics 1987; 4(3):337-350.

27. Yun CS, Javier A, Jennings T, Fisher M, Hira S, Peterson S, Hopkins B, Reich NO, Strouse GF. Nanometal surface energy transfer in optical rulers, breaking the FRET barrier. Journal of the American Chemical Society 2005; 127(9):3115-3119.

28. Persson BNJ, Lang ND. Electron-Hole-Pair Quenching of Excited-States Near A Metal. Physical Review B 1982; 26(10):5409-5415.

29. Danos L, Greef R, Markvart T. Efficient fluorescence quenching near crystalline silicon from Langmuir-Blodgett dye films. Thin Solid Films 2008; 516(20):7251-7255.

30. Vijgenboom E, Busch JE, Canters GW. In vivo studies disprove an obligatory role of azurin in denitrification in Pseudomonas aeruginosa and show that azu expression is under control of RpoS and ANR. Microbiology-Sgm 1997; 143:2853-2863.

31. Schmauder R, Alagaratnam S, Chan C, Schmidt T, Canters GW, Aartsma TJ. Sensitive detection of the redox state of copper proteins using fluorescence. Journal of Biological Inorganic Chemistry 2005; 10(6):683-687.

32. Kuznetsova S, Zauner G, Schmauder R, Mayboroda OA, Deelder AM, Aartsma TJ, Canters GW. A Forster-resonance-energy transfer-based method for fluorescence detection of the protein redox state. Analytical Biochemistry 2006; 350(1):52-60.

33. Cui XD, Primak A, Zarate X, Tomfohr J, Sankey OF, Moore AL, Moore TA, Gust D, Harris G, Lindsay SM. Reproducible measurement of single-molecule conductivity. Science 2001; 294(5542):571-574.

34. See supplementary material at XXXX for additional figures illustrating the features of azurin molecules on a C10d mixed SAM on gold and the difference in roughness between a 10 nm and a 100nm Au film

35. Nar H, Messerschmidt A, Huber R, Vandekamp M, Canters GW. Crystal-Structure Analysis of Oxidized Pseudomonas-Aeruginosa Azurin at Ph 5.5 and Ph 9.0 - A Ph-Induced Conformational Transition Involves A Peptide-Bond Flip. Journal of Molecular Biology 1991; 221(3):765-772.

36. Wink T, vanZuilen SJ, Bult A, vanBennekom WP. Self-assembled monolayers for biosensors. Analyst 1997; 122(4):R43-R50.

37. Love JC, Estroff LA, Kriebel JK, Nuzzo RG, Whitesides GM. Self-assembled monolayers of thiolates on metals as a form of nanotechnology. Chemical Reviews 2005; 105(4):1103-1169.

38. Qu D, Kim BC, Lee CWJ, Uosaki K. 1,n-Alkanedithiol (n=2, 4, 6, 8, 10) Self-Assembled Monolayers on Au(111): Electrochemical and Theoretical Approach. Bulletin of the Korean Chemical Society 2009; 30(11):2549-2554.

39. Benda A, Hof M, Wahl M, Patting M, Erdmann R, Kapusta P. TCSPC upgrade of a confocal FCS microscope. Review of Scientific Instruments 2005; 76(3).

40. Zhang J, Lakowicz JR. Metal-enhanced fluorescence of an organic fluorophore using gold particles. Optics Express 2007; 15(5):2598-2606.

41. Ray K, Zhang J, Lakowicz JR. Fluorescence lifetime correlation spectroscopic study of fluorophore-labeled silver nanoparticles. Analytical Chemistry 2008; 80(19):7313-7318.

42. Heering HA, Canters GW. Activating Redox Enzymes through Immobilisation and Wiring. In: Davis J. J. (ed) Engineering the Bioelectronic Interface: Applications to Analyte Biosensing and Protein Detection. Royal Society of Chemistry: 2009; pp 119-152.

43. O'Dwyer C, Gay G, de Lesegno BV, Weiner J. The nature of alkanethiol self-assembled monolayer adsorption on sputtered gold substrates. Langmuir 2004; 20(19):8172-8182.

44. Yao X, Wang JX, Zhou FM, Wang J, Tao NJ. Quantification of redox-induced thickness changes of 11-ferrocenylundecanethiol self-assembled monolayers by electrochemical surface plasmon resonance. Journal of Physical Chemistry B 2004; 108(22):7206-7212.

45. Kelly KL, Coronado E, Zhao LL, Schatz GC. The optical properties of metal nanoparticles: The influence of size, shape, and dielectric environment. Journal of Physical Chemistry B 2003; 107(3):668-677.

46. Aroca R, Kovacs GJ, Jennings CA, Loutfy RO, Vincett PS. Fluorescence Enhancement from Langmuir-Blodgett Monolayers on Silver Island Films. Langmuir 1988; 4(3):518-521.

47. Chumanov G, Sokolov K, Gregory BW, Cotton TM. Colloidal Metal-Films As A Substrate for Surface-Enhanced Spectroscopy. Journal of Physical Chemistry 1995; 99(23):9466-9471.

48. Biteen JS, Pacifici D, Lewis NS, Atwater HA. Enhanced radiative emission rate and quantum efficiency in coupled silicon nanocrystal-nanostructured gold emitters. Nano Letters 2005; 5(9):1768-1773.

49. Shen H, Lu GW, Ou MG, Marquette CA, Ledoux G, Roux S, Tillement O, Perriat P, Cheng BL, Chen ZH. How the morphology of biochips roughness increases surface-enhanced chemiluminescence. Chemical Physics Letters 2007; 439(1-3):105-109.

50. Wokaun A, Lutz HP, King AP, Wild UP, Ernst RR. Energy-Transfer in Surface Enhanced Luminescence. Journal of Chemical Physics 1983; 79(1):509-514.

51. Sokolov K, Chumanov G, Cotton TM. Enhancement of molecular fluorescence near the surface of colloidal metal films. Analytical Chemistry 1998; 70(18):3898-3905.

52. Aussenegg FR, Leitner A, Lippitsch ME, Reinisch H, Riegler M. Novel Aspects of Fluorescence Lifetime for Molecules Positioned Close to Metal-Surfaces. Surface Science 1987; 189:935-945.

53. Sapsford KE, Berti L, Medintz IL. Materials for fluorescence resonance energy transfer analysis: Beyond traditional donor-acceptor combinations. Angewandte Chemie-International Edition 2006; 45(28):4562-4588.